Solid State Ionics 324 (2018) 33–39

Contents lists available at ScienceDirect

Solid State Ionics

journal homepage: www.elsevier.com/locate/ssi

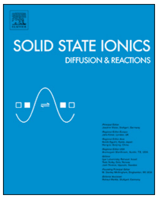

Structural changes in electrochemically cycled $LiMn_{0.7}Fe_{0.3}PO_4$

N.D. Trinh[a], Z.W. Ai[a], G. Liang[b], S.B. Schougaard[a,*]

[a] Dep. of Chemistry, NanoQAM, Université du Québec à Montréal, Quebec Centre for Functional Materials, Case Postale 8888 Succ. Centre-ville, Montréal, Québec H3C 3P8, Canada
[b] Johnson Matthey Battery Materials Ltd, 280 Ave. Liberté, Candiac, Québec J5R 6X1, Canada

ARTICLE INFO

Keywords:
Lithium-ion battery
Phase diagram
Quasi equilibrium
Solid solution
Olivine
Heterosite

ABSTRACT

$Li_{(1-x)}Mn_{0.7}Fe_{0.3}PO_4$ ($0.00 \le x \le 1.0$) samples, obtained by electrochemical cycling, were investigated by powder X-ray diffraction (XRD) and Fourier-transform infrared spectroscopy (FTIR). The purpose of this work is to map phase transition information for samples at quasi equilibrium *i.e.* after a long relaxation time. The required high accuracy solid Li^+ content was determined by atomic emission using the standard addition method. From XRD analysis of the charging cycle samples, the phase diagram was shown to exhibit a solid solution ($0 \le x \le 0.42$), followed by a two phases system exhibiting both *olivine* and *heterosite* structures ($0.42 < x \le \sim 0.91$) and finally above $x \sim 0.91$ the *olivine* phase is no longer detectable. The same basic pattern was found during the discharge process. Combined analysis of FTIR spectra and XRD data showed a strong correlation, where vibration bands at 690 and 600 cm^{-1} could be uniquely attributed to the *heterosite* structure.

1. Introduction

The electric vehicles use is constantly growing, leading to a reduction of greenhouse gas emissions as a positive consequence [1]. However, to become even more attractive, this technology needs further improvement. One of the main remaining issues is the autonomy *i.e.* the distance that the electric vehicle can reach with a fully charged battery. To address this challenge, intensive efforts are made to increase the energy density [2]. As an example, lithium iron phosphate, $LiFePO_4$, provides a theoretical energy density of ~586 $Wh\,kg^{-1}$ *vs* a lithium anode. This however may be insufficient for long range transportation [3]. One improvement strategy is partial substitution of the Fe^{2+}/Fe^{3+} redox couple by another 3*d* transition metal with a higher redox potential [4]. In this context $LiMn_yFe_{1-y}PO_4$ represents a promising candidate because of the possible combination of the high rate electrochemical performance of $LiFePO_4$ and the higher operational voltage from the Mn^{2+}/Mn^{3+} redox couple (4.10 V *vs* Li/Li^+) [5]. However, substituted materials necessary imply modifications in the intrinsic properties, which leads to different phase transformation compared to pure $LiFePO_4$ [6].

The equilibrium reactions of delithiation and relithiation of $LiFePO_4$ occurs *via* a two phase mechanism. The two phases are described as Li-rich (*olivine*) and Li-poor (*heterosite*), with solid solutions formed close to both end members of the Li_xFePO_4 phase diagram [7,8]. According to the Domino-cascade model, the Li^+ diffusion only occurs along the *b* axis of the unit cell, while the boundary moves along the *a* axis [9]. In contrast to this model, a non-equilibrium solid solution mechanism is possible, demonstrated by both theoretical calculations and experimental observations [10–12]. This latter mechanism is kinetically favorable because the lithium ion is free to move inside the structure, avoiding both lattice strain at the $LiFePO_4/FePO_4$ interface and the formation of nucleation sites [13]. In comparison, the $LiMn_yFe_{1-y}PO_4$ dynamic electrochemical response and proposed mechanisms have a strong dependence on Mn/Fe ratio [14–20]. Consequently, the target here is *ex situ* X-ray diffraction (XRD) of a quasi equilibrium state *i.e.* after a long time relaxation period, as a point of comparison for dynamic data. As such, we expand on the work of Yamada et al. who performed structural analysis of chemically delithiated $LiMn_yFe_{1-y}PO_4$ compositions [21,22]. We here use an electrochemical technique to eliminate possible Mn dissolution by oxidation using NO_2^+, and by adding Fourier-transform infrared spectroscopy (FTIR) to examine the local structure evolution.

2. Experimental section

2.1. Material characterization

Carbon coated $LiMn_{0.7}Fe_{0.3}PO_4$ (LMFP) powder was provided by Johnson Matthey Battery Materials Ltd. (Candiac). The carbon content was determined by CHNS elemental analysis (EAS1108, Fisons Instruments). Transmission electron microscopy (TEM) was performed with a JEOL JEM-2100F and an acceleration voltage of 200 keV. TEM

---

* Corresponding author.
E-mail address: schougaard.steen@uqam.ca (S.B. Schougaard).

https://doi.org/10.1016/j.ssi.2018.05.018
Received 4 January 2018; Received in revised form 4 May 2018; Accepted 16 May 2018

samples were prepared by suspending powders in methanol using an ultrasonic bath, before deposition onto a carbon grid. The powder was characterized by *ex situ* X-ray diffraction using a Phillips X'Pert Pro diffractometer with Cu K_α radiation (1.5418 Å). The current and voltage were 40 mA and 50 kV respectively with a step size of 0.015° s^{-1} in the 2θ range of 15–75°. 10% m/m silicon powder 1–5 µm (Alfa Aesar 99.5%) was mixed into the sample, as an internal standard. Rietveld refinement was performed Fullprof 3.2 software [23]. Fourier-transform infrared spectroscopy (FTIR) was performed on a Nexus 670 FTIR Nicolet: A mixture of ~1 mg of the material and 300 mg of KBr (Fischer Scientific) was ground to a homogeneous powder and pressed to form a pellet of ~1 mm thickness. The spectral range of 1500–300 cm^{-1} was probed with a total of 32 scans combined for each spectrum. The lithium content in the solid samples was determined by dissolving 8–10 mg of the electrode powder in 20 mL of boiling concentrated nitric acid (Caledon). The mixture was allowed to react for 1 h or until complete dissolution. The solution was passed through a 20 µm filter to remove residual carbon particles. The sample was diluted to fit within a calibration curve spanning concentrations between 0.1 and 0.6 ppm of Li^+ (Alfa Aesar standard solution). The acquisition was performed using a Varian SpectrAA 220 FS at 670.8 nm wavelength. Standard addition method was used to quantify the lithium concentration in the sample mainly to avoid possible interference from the electrode matrix. Inductive coupled plasma spectroscopy (ICP, Thermo 6500 Dual View) is used to quantify the iron, manganese and phosphorous contents of the starting material at 259.9 nm, 257.6 nm and 177.4 nm respectively. The sample was diluted to fit in the calibration curve of the respective element spanning from 0.5 to 5 ppm for the Fe, Mn and P elements, in a 5% HNO_3 medium (SpectraPure, Fisher Alfa Aesar and standard solutions respectively).

2.2. *Electrochemistry procedure*

The electrodes were made by preparing a slurry composed of 80% of active material, 12% of acetylene black (MTI Corp.) and 8% of PVDF (Kynar KF Polymer W#1100) in *N*-methylpyrrolidone (NMP, Alfa Aesar 99.5%). The mixture was stirred using a roller mill for 24 h to obtain a uniform suspension before casting on an aluminum current collector (MTI Corp.) with a film applicator (BYK-Gardner USA) adjusted to 90 µm. The composite electrode was dried at 60 °C at atmospheric pressure for 2 h and then under vacuum at 60 °C for 24 h. From the obtained electrode, rectangles of specific dimension (6 cm × 3.5 cm) were cut. The upper portion of the composite was scraped from the electrode (2 cm), freeing space for electrical connection. The geometric area of the electrodes immerged in the electrolyte was estimated at 14 cm^2. The average thickness (~70 µm) of the electrodes was measured by a Mitutoyo 7326S thickness gage, for an active material loading of 1.1 to 1.4 mg cm^{-2}.

The electrochemical delithiation/relithiation was performed in a home made three electrodes cell using a Bio-Logic VMP3 potentiostat. The electrochemical cell was composed of an inner fritted container accommodating the reference, Li foil (Alfa Aesar 99.95%) soaked in electrolyte behind Vycor frit, and working electrodes in 0.5 M $LiClO_4$ (Alfa Aesar 99.8%) in propylene carbonate (Sigma Aldrich 99.9%). A Li foil (1.5 cm × 6 cm), placed directly underneath the fritted inner container in the outer beaker served as the counter electrode. All the experiments were performed in an argon filled gloves box.

For the charging process, a constant current at C/10 was imposed with a 4.35 V *vs* Li/Li^+ upper cut-off. Charging was carried out for times varying between 30 min to 10 h, to obtain various Li^+ contents in $Li_{(1-x)}Mn_{0.7}Fe_{0.3}PO_4$ ($0.00 < x \leq 1.0$). To obtain high values of x, a constant potential at 4.35 V *vs* Li/Li^+ was imposed. A similar procedure was used to obtain samples from the discharge cycle, using a C/10 constant current. Finally, the working electrode was removed from the reactional media and rinsed with anhydrous acetonitrile (Sigma Aldrich 99.9%) in the glove box. The electrodes were dried at 60 °C under vacuum for 24 h before further use. The electrode composition was scratched off from the current collector and ground to obtain a uniform powder.

To verify the electrochemical activity of the active material, CR2032-type coin cells were assembled using metallic lithium (Alfa Aesar 99.9%) as the negative electrode, and a disk electrode (d = 14 mm) cut from a rectangle electrodes detailed above as the positive electrode. The electrolyte was 1 M $LiPF_6$ in a 1:1 ethylene carbonate (EC) and dimethyl carbonate (DMC) mixture (Novalyte Technologies) and porous polypropylene (Celgard 2500) was used as the separator. The cells were assembled in an argon atmosphere glove box. Electrochemical testing was performed by galvanostatic cycling using a C/20 current between 2.2 and 4.3 V *vs* Li/Li^+ at room temperature, and a BST8-MA (MTI Ltd.) battery analyzer. An open circuit rest period was imposed during 1 h at charge reversal.

3. Results and discussion

3.1. *Starting material* $LiMn_{0.7}Fe_{0.3}PO_4$

TEM micrograph showed the samples to be composed of agglomerates of semi-spherical particles with diameter of ~100 nm (Fig. 1a). High resolution TEM micrograph (Fig. 1b) demonstrated well-defined lattice planes inside the particle and a carbon coating thickness of ~3–4 nm. Elemental analysis showed a carbon content of 1.18 m/m%.

The crystalline structure was confirmed by powder X-ray diffraction

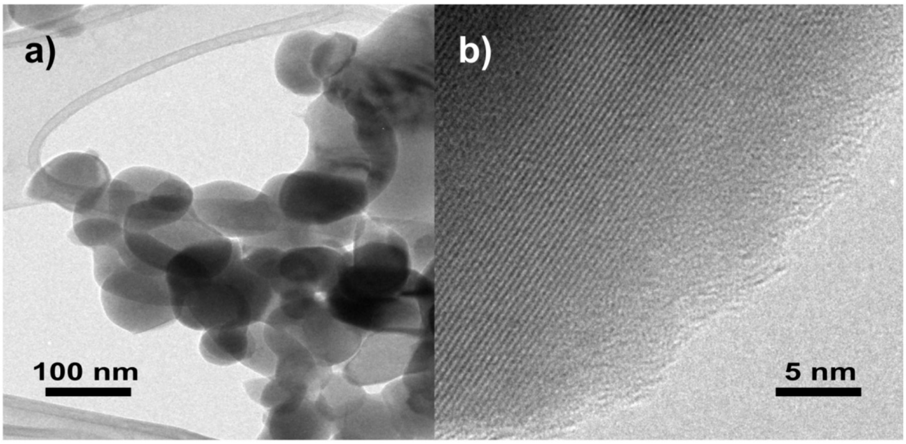

Fig. 1. a) TEM micrograph showing the morphology and particle size and b) HRTEM micrograph of a single particle showing the thickness of the carbon layer and the lattice fringes.